JTTEE5 15:348-355
DOI: 10.1361/105996306X124347
1059-9630/$19.00 © ASM International

Peer Reviewed

Effect of Grit-Blasting on Substrate Roughness and Coating Adhesion

Dominic J. Varacalle, Jr., Donna Post Guillen, Douglas M. Deason, William Rhodaberger, and Elliott Sampson

(Submitted August 15, 2005; in revised form June 16, 2006)

Statistically designed experiments were performed to compare the surface roughness produced by grit blasting A36/1020 steel using different abrasives. Grit blast media, blast pressure, and working distance were varied using a Box-type statistical design of experiment (SDE) approach. The surface textures produced by four metal grits (HG16, HG18, HG25, and HG40) and three conventional grits (copper slag, coal slag, and chilled iron) were compared. Substrate roughness was measured using surface profilometry and correlated with operating parameters. The HG16 grit produced the highest surface roughness of all the grits tested. Aluminum and zinc-aluminum coatings were deposited on the grit-blasted substrates using the twin-wire electric arc (TWEA) process. Bond strength of the coatings was measured with a portable adhesion tester in accordance with ASTM standard D 4541. The coatings on substrates roughened with steel grit exhibit superior bond strength to those prepared with conventional grit. For aluminum coatings sprayed onto surfaces prepared with the HG16 grit, the bond strength was most influenced by current, spray distance, and spray gun pressure (in that order). The highest bond strength for the zinc-aluminum coatings was attained on surfaces prepared using the metal grits.

Keywords bond strength, grit blasting, statistical design of experiments, substrate preparation, surface roughness, twin-wire electric arc

1. Introduction

Thermal spray coatings are currently being used in over 50 industries for a variety of applications. Aluminum and zinc-aluminum (Zn-Al) coatings are extensively used for the corrosion protection of iron (Fe) and steel in a wide range of environments and have been shown to provide long-term protection (over 20 years) for both marine and industrial service (Ref 1). This study was specifically undertaken to examine the effect of grit blasting and subsequent thermal spray coating of bridges constructed with A36 steel. Adhesion of the thermal spray coating to the steel substrate is critical to the successful performance of these coatings, and most thermal spray coatings bond to the substrate primarily by mechanical bonding. Thus, it is crucial that the substrate be properly prepared to ensure maximum coating bond strength (Ref 2).

Surface cleanliness and roughness are the most important factors affecting adhesion (Ref 3). Properly cleaned and roughened surfaces provide the critical interface upon which the first molten or plasticized particles strike when using thermal spray processes. A properly prepared surface provides enhanced metal-to-metal contact for interatomic and metallurgical interaction between the substrate and the sprayed particles. Roughening significantly increases surface area for particle-to-substrate contact by increasing atomic and metallurgical interaction, and also provides many opportunities for mechanical interlocking. Abrasive blasting is conducted to prepare substrates prior to the application of thermal spray coatings by removing contaminants and roughening the surface to provide the surface profile necessary for good adhesion of the thermal spray coating to the substrate. The surface profile consists of a pattern of peaks and valleys etched into the steel resulting from the impingement of high-velocity abrasive particles. The substrate should be cleaned following grit blasting to remove residual dust by either rinsing with a solvent or air drying using clean, dry compressed air. It is important that the prepared surface is coated as soon as possible after preparation to prevent surface oxidation/contamination that can lead to coating failures (Ref 4). This is typically done within 2 h.

Alumina, silica sand, steel, Fe, copper (Cu) slag, and silicon carbide are often used as abrasive grit. Ceramic grits are commonly used on large exterior structures where recovery of the grit is impractical. Metal grit is most commonly used on bridges as well as Cu slag, Fe, and coal slag. Metal grit is typically reclaimed in bridge grit blasting for economic and environmental reasons. For any application, consideration should be given to the substrate materials in the selection of grit types. Traces of residual grit may adversely affect some coatings. Alumina, sand, and especially silicon carbide may embed in softer metals such as Al, Cu, and their alloys. For these metals, lower working air pressures are typically used to minimize embedding. For typical applications, grit-blasting air pressure varies from 207 to 827 kPa (30 to 120 psia) with a wide range of working distances of 50 to 914 mm (2 to 36 in.). Nozzle sizes are generally 3 to 16 mm (0.125 to 0.625 in.) in diameter. The blasting angle to the substrate can vary from 45 to 90° (Ref 5).

Grit sizes can be classified as coarse (2.0 to 0.6 mm/−10 to +30 mesh), medium (1.4 to 0.425 mm/−14 to +40 mesh), and fine (0.60 to 0.18 mm/−30 to + 80 mesh). Properties of the grit

Dominic J. Varacalle, Jr., Vartech, Inc., Idaho Falls, ID; **Donna Post Guillen,** Idaho National Laboratory, Idaho Falls, ID; **Douglas M. Deason,** U.S. Army Space and Missile Defense Command, Huntsville, AL; **William Rhodaberger,** Ervin Industries, Ann Arbor, MI; and **Elliott Sampson,** Praxair Tafa, Bow, NH. Contact e-mail: Donna.Guillen@inl.gov.

media that affect surface preparation include grit size, type, and hardness. For a given nozzle geometry, relevant process parameters include air pressure, working nozzle distance, and angle. Typically for coatings that are to be used in the as-sprayed condition, coarse grit is used for coatings exceeding 0.0254 cm (10 mils) for best adhesion, medium grit is used for smoother finishes of coatings less than 0.0254 cm (10 mils) with good adhesion, and fine grit is used for the smoothest finishes on coatings less than 0.0254 cm (10 mils) for fair adhesion. Thus, the selection of the grit size is partially determined by the required coating thickness and considered on an individual basis for each application.

Statistical design of experiments (SDE) has been rigorously developed over the past 80 years by numerous scientists including Sir Ronald Fisher (Ref 6). The motivation for designing an experiment statistically is to obtain unambiguous results at a minimum cost. Thus, SDE methods are important tools to an engineer wishing to achieve an economical design for a product. These experimental designs constitute a plan for constructively changing the input parameters to determine their effect on the attributes of the product (Ref 7). A variety of SDE strategies are available to obtain statistical information within the selected test matrix. Use of the SDE methodology can optimize surface roughness and coating bond strength by producing insight into the physical mechanisms involved in the preparation of substrates for thermal spraying.

2. Grit-Blast Study

Experiments were conducted to assess the relative effectiveness of the grits and their effect on coating bond strength. The study included: (a) measuring the effect of various abrasives and grit blasting parameters on the surface roughness of A36/1020 steel, (b) comparing the substrate's response to steel abrasives versus conventional abrasives, and (c) testing the bond strength of Twin-Wire Electric Arc (TWEA) sprayed coatings on the grit-blasted substrates. Process parameters for each type of grit were determined using SDE. Aluminum and zinc-aluminum coatings were sprayed onto substrates prepared using the grit blast parameters that produced the optimum roughened surface.

2.1 Experimental Procedure

A modified Econoline (Grand Haven, MI) RA 36-1 grit-blasting device (Ref 8) was used for this study. The Econoline cabinet is rectangular in shape and has a self-contained, recycling, sealed glove box design. It is capable of blasting small pieces, up to 77.5 cm (30.5 in.) in length. The abrasive hopper that is located below the worktable holds between 11.4 and 22.7 kg (25 and 50 lb) of blasting material. The spray gun consists of a 708 lpm (1500 scfh) carbide nozzle and a 708 lpm (1500 scfh) air jet housed in a large bronze gun body. The blasting media is drawn into the gun through a siphon tube connected to the base of the pistol grip. A pressure regulator on the exterior of the cabinet allows the operator to regulate air supply pressure from 69 to 827 kPa (10 to 120 psia). An external dust collector sweeps and filters the air in the cabinet to improve visibility during blasting operations. The grit blasting device was operated manually. To ensure repeatability and consistency in the grit blasting operation, the time spent blasting each substrate was limited to 30 s and a slider platform was utilized to ensure standoff distance and angle.

A Box-type design of experiments (Ref 9) was used to optimize the process parameters for the grit blast equipment. This statistical analysis was accomplished with the use of the Design-Expert software (Ref 10). The design of experiment approach is a powerful tool because it statistically delineates the impact of each process parameter on the measured characteristics across all combinations of the other parameters. The parameters being optimized in the grit-blast studies included working distance (D = 5.1 to 10.2 cm, or 2 to 4 in.), blast pressure (P = 551.6 to 827.4 kPa, or 80 to 120 psia), and blast media. For the grit-blast device of this study, the range of these parameters yielded a wide range of particle velocities at substrate impact. A blasting angle of 90° was used. Previous research has shown that the maximum adhesion strength was obtained using a 90° blasting and spraying angle (Ref 4). The substrates used for the studies were low-carbon steel (A36/1020).

Two sets of grit-blast studies were conducted—one set for the steel grits and the other set for the conventional grits. The factorial design for the metal grit studies is illustrated in Table 1. The range of process parameters for the metal and conventional grits was chosen to attain the widest range of surface texture variability. Each variable has fixed ranges selected to determine the parameter space for surface preparation optimization. Experiments E1 through E52 used Ervin Amasteel (Ann Arbor, MI) HG16, HG18, HG25, and HG40 metal grit. The designator HG indicates a Rockwell hardness of 60+ HRC, and the size of these grits corresponds to the Society of Automotive Engineers (SAE) J444 grit tolerances. A three-level response surface factorial experiment, shown in Table 1, was used. For the varied surface texture parameters, linear and quadratic models yielded the best fit to the data. Experiments C1 through C41 were then conducted with the conventional grit materials: Cu slag (30 mesh), coal slag (30 mesh), and chilled Fe grit (40 mesh). Again, a three-level response surface factorial experiment was used. Linear and quadratic models yielded the best fit to the data.

The substrates were visually examined with a Nikon SMZ-2B (Melville, NY) microscope. The roughened substrates produced by grit blasting with the metal grit appeared to be relatively free from embedded grit or surface scale particles, while the substrates blasted with the slag grits contained some visible embedded grit.

2.2 Roughness Measurements

Surface roughness was measured using a Surftest 301 roughness tester (Mitutoyo Corp., Japan) (Ref 11). The Surftest 301 unit provides digital readout of the measuring conditions and results for a significant number of surface texture parameters including R_a (arithmetic mean deviation of the profile), R_q (RMS deviation of the profile), R_{3z} (mean peak-to-valley height), R_t (maximum peak to valley height), R_y (maximum peak to valley height), R_z (average peak to valley height), R_p (maximum profile peak height), and P_c (peak count). R_z was used for the primary roughness measurement since it most closely matches ANSI standard B46.1 (Ref 12) (i.e., the average deviation from the

Table 1 Full-factorial design of experiment matrix for HG grit roughness study

E No.	Distance (*D*), level/cm/in.	Pressure (*P*), level/kPa/psia	Grit type, level/type	E No.	Distance (*D*), level/cm/in.	Pressure (*P*), level/kPa/psia	Grit type, level/type
1	1/5.08/2	1/551.6/80	1/HG16	27	1/5.08/2	1/551.6/80	3/HG25
2	2/7.62/3	1/551.6/80	1/HG16	28	2/7.62/3	1/551.6/80	3/HG25
3	3/10.16/4	1/551.6/80	1/HG16	29	3/10.16/4	1/551.6/80	3/HG25
4	1/5.08/2	2/689.5/100	1/HG16	30	1/5.08/2	2/689.5/100	3/HG25
5	2/7.62/3	2/689.5/100	1/HG16	31	2/7.62/3	2/689.5/100	3/HG25
6	3/10.16/4	2/689.5/100	1/HG16	32	3/10.16/4	2/689.5/100	3/HG25
7	1/5.08/2	3/827.4/120	1/HG16	33	1/5.08/2	3/827.4/120	3/HG25
8	2/7.62/3	3/827.4/120	1/HG16	34	2/7.62/3	3/827.4/120	3/HG25
9	3/10.16/4	3/827.4/120	1/HG16	35	3/10.16/4	3/827.4/120	3/HG25
10	2/7.62/3	2/689.5/100	1/HG16	36	2/7.62/3	2/689.5/100	3/HG25
11	2/7.62/3	2/689.5/100	1/HG16	37	2/7.62/3	2/689.5/100	3/HG25
12	2/7.62/3	2/689.5/100	1/HG16	38	2/7.62/3	2/689.5/100	3/HG25
13	2/7.62/3	2/689.5/100	1/HG16	39	2/7.62/3	2/689.5/100	3/HG25
14	1/5.08/2	1/551.6/80	2/HG18	40	1/5.08/2	1/551.6/80	4/HG40
15	2/7.62/3	1/551.6/80	2/HG18	41	2/7.62/3	1/551.6/80	4/HG40
16	3/10.16/4	1/551.6/80	2/HG18	42	3/10.16/4	1/551.6/80	4/HG40
17	1/5.08/2	2/689.5/100	2/HG18	43	1/5.08/2	2/689.5/100	4/HG40
18	2/7.62/3	2/689.5/100	2/HG18	44	2/7.62/3	2/689.5/100	4/HG40
19	3/10.16/4	2/689.5/100	2/HG18	45	3/10.16/4	2/689.5/100	4/HG40
20	1/5.08/2	3/827.4/120	2/HG18	46	1/5.08/2	3/827.4/120	4/HG40
21	2/7.62/3	3/827.4/120	2/HG18	47	2/7.62/3	3/827.4/120	4/HG40
22	3/10.16/4	3/827.4/120	2/HG18	48	3/10.16/4	3/827.4/120	4/HG40
23	2/7.62/3	2/689.5/100	2/HG18	49	2/7.62/3	2/689.5/100	4/HG40
24	2/7.62/3	2/689.5/100	2/HG18	50	2/7.62.3	2/689.5/100	4/HG40
25	2/7.62/3	2/689.5/100	2/HG18	51	2/7.62/3	2/689.5/100	4/HG40
26	2/7.62/3	2/689.5/100	2/HG18	52	2/7.62/3	2/689.5/100	4/HG40

Table 2 Maximum and minimum measured values of the surface texture parameters for the seven grits of this study

	R_a		R_q		R_{3z}		R_t		R_y		R_z		$R_{p\ max}$		
Grit type	µm	mil	µm	mil	µm	mil	µm	mil	µm	mil	µm	mil	µm	mil	P_c
Maximum measured value															
HG16	16.8	0.66	21.3	0.84	65.0	2.56	138.7	5.46	120.7	4.75	101.1	3.98	73.7	2.90	119
HG18	15.0	0.59	19.3	0.76	55.6	2.19	130.8	5.15	121.9	4.80	96.5	3.80	64.3	2.53	142
HG25	13.7	0.54	17.0	0.67	55.9	2.20	113.8	4.48	107.2	4.22	84.1	3.31	59.4	2.34	147
HG40	10.9	0.43	13.5	0.53	43.9	1.73	88.6	3.49	79.0	3.11	63.2	2.49	48.5	1.91	185
Minimum measured value															
HG16	11.9	0.47	15.5	0.61	45.0	1.77	101.3	3.99	93.7	3.69	74.4	2.93	47.0	1.85	79
HG18	11.4	0.45	15.0	0.59	47.8	1.88	92.2	3.63	86.9	3.42	77.2	3.04	42.2	1.66	104
HG25	10.2	0.40	12.7	0.50	44.7	1.76	72.9	2.87	72.4	2.85	62.0	2.44	34.0	1.34	99
HG40	7.9	0.31	9.7	0.38	37.1	1.46	51.6	2.03	51.6	2.03	47.0	1.85	22.6	0.89	140
Maximum measured value															
Cu	11.9	0.47	15.2	0.60	48.5	1.91	106.9	4.21	102.1	4.02	78.5	3.09	56.2	2.21	163
Coal	10.4	0.41	13.5	0.53	43.5	1.71	101.3	3.99	94.0	3.70	73.2	2.88	46.0	1.81	193
Fe	8.4	0.33	10.4	0.41	38.1	1.50	76.2	3.00	69.1	2.72	57.7	2.27	35.6	1.40	178
Minimum measured value															
Cu	9.4	0.37	12.2	0.48	40.1	1.58	69.6	2.74	68.1	2.68	62.5	2.46	32.8	1.29	122
Coal	7.1	0.28	9.1	0.36	32.3	1.27	59.7	2.35	55.6	2.19	49.5	1.95	26.7	1.05	137
Fe	6.9	0.27	8.6	0.34	31.5	1.24	55.6	2.19	53.6	2.11	46.0	1.81	21.3	0.84	127

mean line of elevation through the surface asperities). Specifications for the Surftest 301 tester include: stylus measuring traverse speed of 0.5 mm/s (0.02 in./s), total number of samples of 1000 points/span, cutoff value of 0.25 mm (0.01 in.), sampling lengths of 0.25, 0.8, 2.5, and 8 mm (0.01, 0.03, 0.1, and 0.3 in.), and a sampling span of 0.25 µm. The stylus material is diamond with a tip radius of 5 µm. The detecting mode uses the differential inductance method.

The maximum and minimum measured values for the aforementioned surface texture parameters are presented in Table 2 for all the grit types used in this study. R_a and R_q represent the deviations of the grit-blasted profiles. The larger the value of R_a and R_q, the higher the skewness of the profile. Higher values of R_a and R_q indicate a greater surface area for contact in the *x*-*y* dimension, and thus enhanced coating bond strength. Higher values of the profile height (i.e., *z* dimension), represented by the surface texture parameters R_t, R_{3z}, R_y, R_z, and $R_{p\ max}$ indicate a greater total surface area, which would also enhance coating bond strength. Higher values of P_c are indicative of a higher profile peak density.

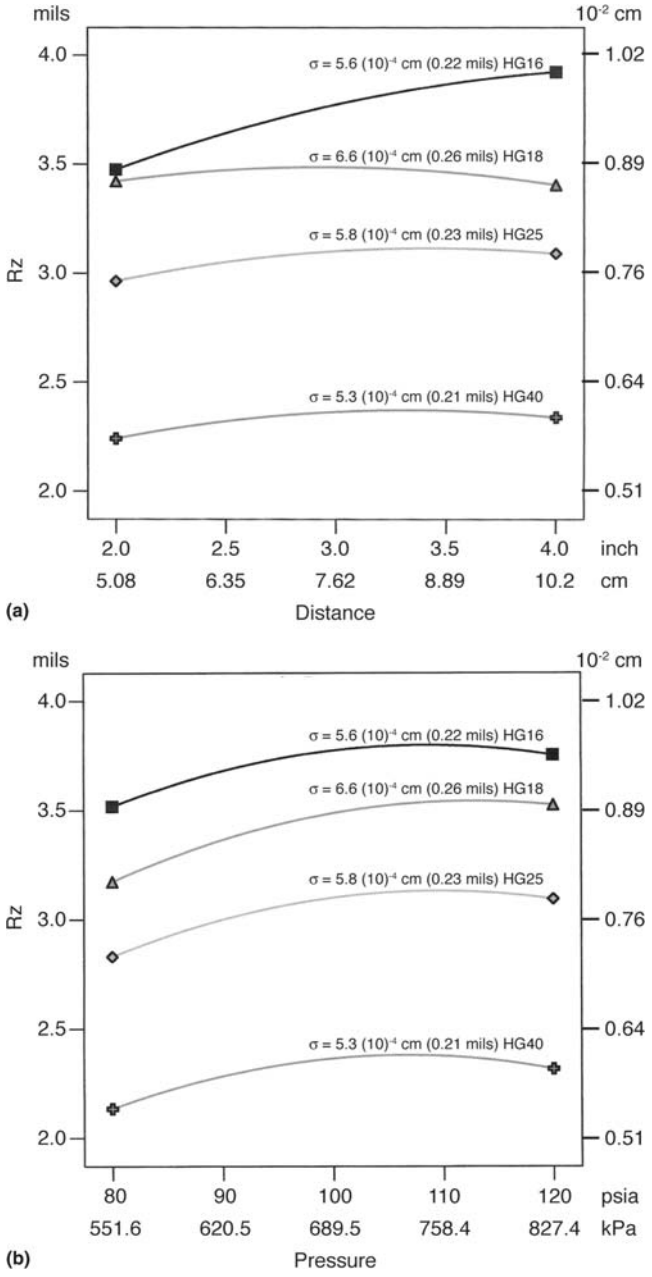

Fig. 1 Surface roughness produced using steel grit as a function of (a) working distance at a constant pressure of 689.5 kPa (100 psia) and (b) pressure and at a constant working distance of 7.62 cm (3 in.)

Figures 1(a) and (b) illustrate the results of the steel grit study. The measured R_z values for the four steel grits at a constant pressure (689.5 kPa, or 100 psia) are shown as a function of working distance in Fig. 1(a) and as a function of pressure and constant distance (7.62 cm, 3.0 in.) in Fig. 1(b). In both cases, the HG16 grit produces the maximum R_z profiles, followed by HG18, HG25, and HG40. The maximum R_z for the metal grit ranged from $7.44(10^{-3})$ to $1.01(10^{-2})$ cm (2.93 to 3.98 mils) for the HG16, $7.72(10^{-3})$ to $9.65(10^{-3})$ cm (3.04 to 3.80 mils) for the HG18, $6.20(10^{-3})$ to $8.40(10^{-3})$ cm (2.44 to 3.31 mils) for the HG25, and $4.70(10^{-3})$ to $6.32(10^{-3})$ cm (1.85 to 2.49 mils) for the HG40. The 1σ standard deviation values are listed on the figures.

The surface roughness produced with the HG16 grit was then compared with that produced with the Cu slag, coal slag, and chilled Fe abrasives. Figures 2 and 3 illustrate the results of this study. As shown in Fig. 2, the steel grit HG16 attains a larger Rz profile than the Cu slag, coal slag, and chilled Fe. The response surface plots for roughness R_z are presented as a function of working distance and working pressure for the four abrasives. As illustrated, the HG16 grit (Fig. 2a) produces the maximum R_z roughness ranging from $7.44(10^{-3})$ to $1.01(10^{-2})$ cm (2.93 to 3.98 mils). The R_z roughness for the Cu slag abrasive ranged from $6.25(10^{-3})$ to $7.85(10^{-3})$ cm (2.46 to 3.09 mils) (shown in Fig. 2b), $4.95(10^{-3})$ to $7.32(10^{-3})$ cm (1.95 to 2.88 mils) for coal slag (shown in Fig. 2c), and $4.60(10^{-3})$ to $5.77(10^{-3})$ cm (1.81 to 2.27 mils) for chilled Fe grit (shown in Fig. 2d). The trends for increasing R_z roughness for coal slag and chilled Fe grit follow the trends exhibited by the HG16 grit—i.e., R_z increases as the working distance increases, with the roughness reaching a maximum at intermediate pressure (i.e., ~689.5 kPa, or 100 psia).

Strictly defined, R_a is the root mean square average of the profile height deviations taken within the evaluation length and measured from the mean line (Ref 12). Higher R_a values correspond to higher surface areas for the selected profile. As illustrated, the HG16 grit (shown in Fig. 3a) produces the maximum R_a roughness ranging from $1.194(10^{-3})$ to $1.676(10^{-3})$ cm (0.47 to 0.66 mils). The R_a roughness for the Cu slag ranged from $0.94(10^{-3})$ to $1.194(10^{-3})$ cm (0.37 to 0.47 mils) (shown in Fig. 3b), $0.71(10^{-3})$ to $1.04(10^{-3})$ cm (0.28 to 0.41 mils) for coal slag (shown in Fig. 3c), and $0.69(10^{-3})$ to $0.84(10^{-3})$ cm (0.27 to 0.33 mils) for chilled Fe grit (shown in Fig. 3d). The trends for increasing R_a roughness for Cu slag, coal slag, and chilled Fe grit follow the trends exhibited by the HG16 grit—R_a increases as the working distance and pressure increases, with the roughness reaching a maximum at maximum pressure and distance.

As illustrated in Table 2, the trends evidenced for R_z are also seen for the parameters R_a, R_q, R_{3z}, R_t, R_y, and $R_{p\,max}$. The HG16 grit attained higher measured values for all of these surface texture parameters. The measured values for P_c, the profile density, indicate higher values for smaller grit sizes. The coal slag has the highest profile density value, followed by HG40, chilled Fe, Cu slag, HG25, HG18, and HG16. Using the measured combination of average maximum profile height (R_z), average maximum profile skewness (R_a), and average profile peak density value (P_c), normalized surface areas were calculated. Assuming the sawtooth profiles are circular cones, maximum surface area would be achieved for HG16, followed by HG18, HG25, Cu slag, coal slag, HG40, and chilled Fe. The normalized surface area factor relative to chilled Fe (i.e., lowest calculated surface area) is 5.4 for HG16, 4.9 for HG18, 3.1 for HG25, 1.4 for HG40, 2.6 for Cu slag, 1.6 for coal slag, and 1.0 for chilled Fe. This indicates that HG16 could have twice the surface area of the coal slag despite the fact that the coal slag in this study had the highest value of P_c.

2.3 SDE Results

Once the effect of each process parameter was quantified, the levels of the parameters that led to a minimum or maximum of the particular response were determined. Graphical procedures based on normal probability plots were used to choose an appro-

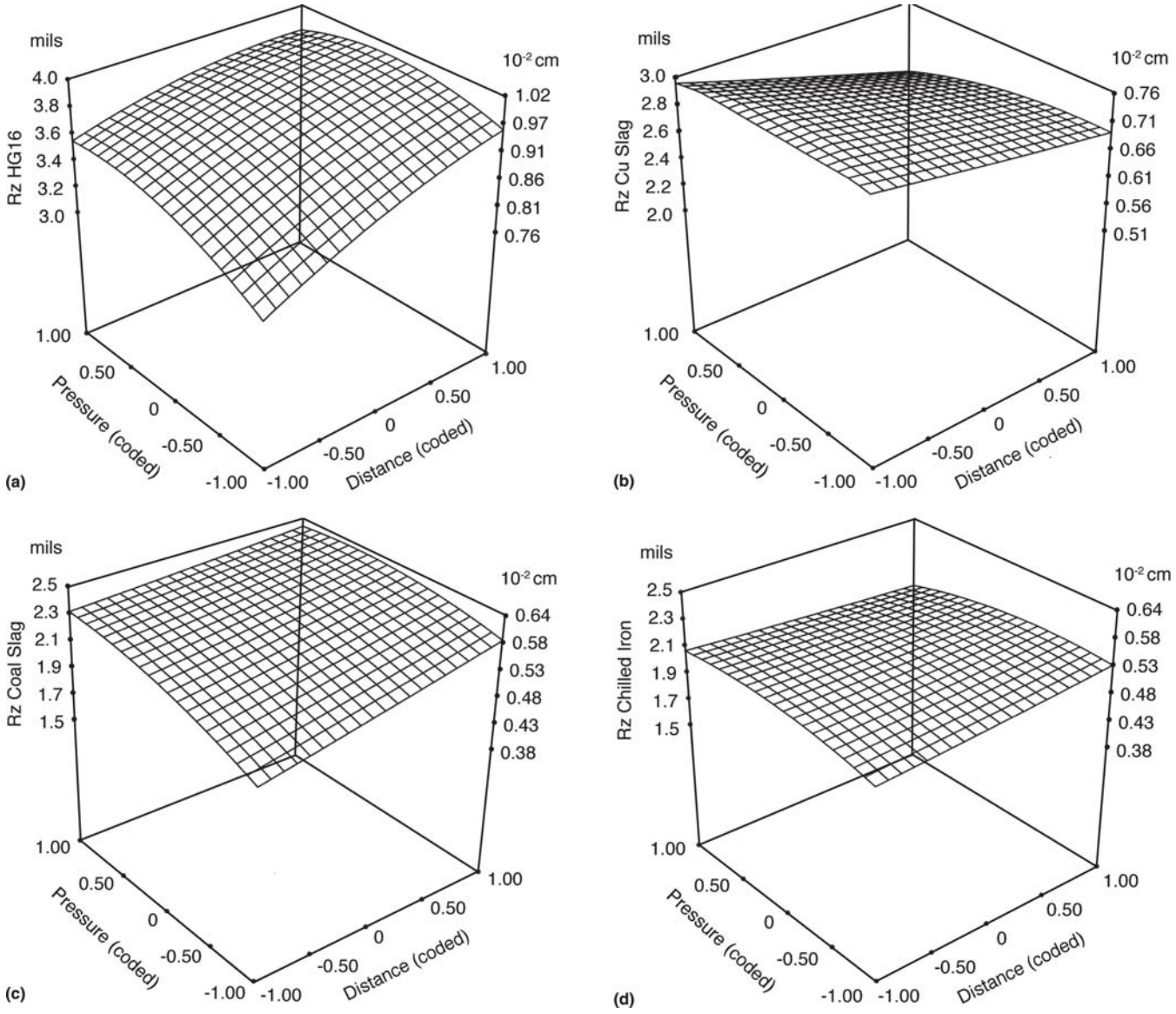

Fig. 2 R_z roughness comparison of (a) HG16, (b) Cu slag, (c) coal slag, and (d) chilled Fe grit. Distance: coded, −1.0 to 1.0; actual, 5.1 to 10.2 cm (2.0 to 4.0 in.). Pressure coded: −1.0 to 1.0; actual, 551.6 to 827.4 kPa (80.0 to 120.0 psia)

priate regression model for each roughness response. Once this analysis was completed, the analysis of variance (ANOVA) calculations were conducted for each response. The statistical values of the *F* value (i.e., the comparison of the treatment variance with the error variance), the probability of a larger *F* value (i.e., the probability that the model terms are null), the predicted residual sum of squares (PRESS) value (i.e., how well the model fits each point in the design), and the coefficient of variation (i.e., a measure of residual variation of the data relative to the size of the mean) were investigated. Once these values yielded robust results, equations were generated that yielded the response surface plots for each surface texture parameter. The equations for the R_z roughness (in cm) of each grit, as a function of the process variables (i.e., pressure and standoff distance) are listed in Eqs. 1 through 7. These equations were used to generate the surface plots shown in Fig. 2(a) to (d) and 3(a) to (d).

$$\text{HG16: } R_z = -7.65(10)^{-3} + 2.90(10)^{-3}{*}D + 2.29(10)^{-4}{*}\text{P} - 1.88(10)^{-4}{*}D^2 - 8.76(10)^{-7}{*}P^2 + 1.20(10)^{-5}{*}D{*}P \quad \text{(Eq 1)}$$

$$\text{HG18: } R_z = -7.37(10)^{-3} + 2.29(10)^{-3}{*}D + 2.29(10)^{-4}{*}\text{P} - 1.88(10)^{-4}{*}D^2 - 8.76(10)^{-7}{*}P^2 - 1.19(10)^{-5}{*}D{*}P \quad \text{(Eq 2)}$$

$$\text{HG25: } R_z = -8.33(10)^{-3} + 2.49(10)^{-3}{*}D + 2.29(10)^{-4}{*}P - 1.88(10)^{-4}{*}D^2 - 8.76(10)^{-7}{*}P^2 - 1.20(10)^{-5}{*}D{*}P \quad \text{(Eq 3)}$$

$$\text{HG40: } R_z = -9.58(10)^{-3} + 2.44(10)^{-3}{*}D + 2.24(10)^{-4}{*}P - 1.88(10)^{-4}{*}D^2 - 8.76(10)^{-7}{*}P^2 - 1.20(10)^{-5}{*}D{*}P \quad \text{(Eq 4)}$$

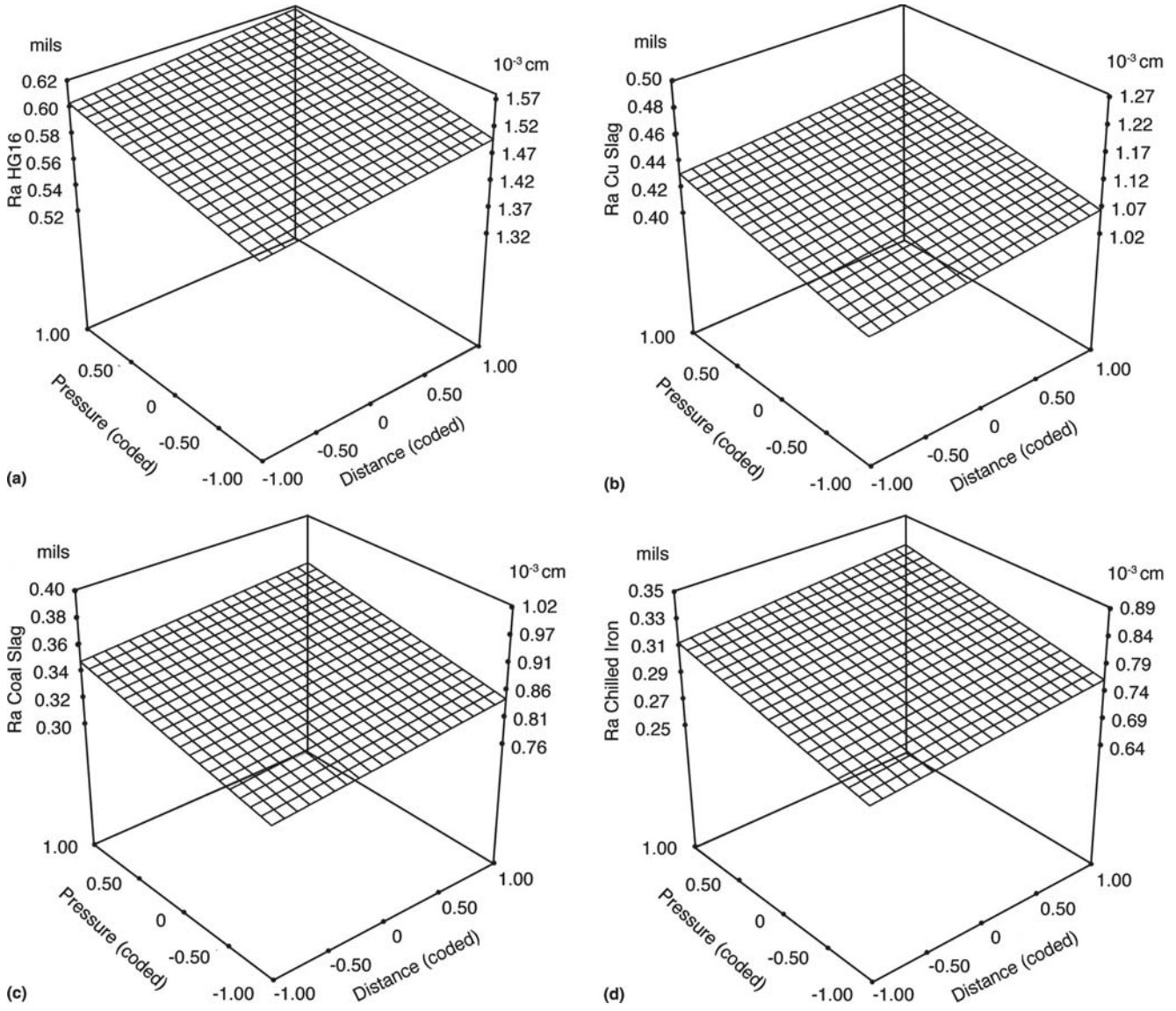

Fig. 3 R_a roughness comparison of (a) HG16, (b) Cu slag, (c) coal slag, and (d) chilled Fe grit. Distance: coded, −1.0 to 1.0; actual, 5.1 to 10.2 cm (2.0 to 4.0 in.). Pressure coded: −1.0 to 1.0; actual, 551.6 to 827.4 kPa (80.0 to 120.0 psia)

$$\text{Copper slag: } R_z = 2.79(10)^{-3} + 2.21(10)^{-4}{*}D + 1.07(10)^{-4}{*}P + 1.10(10)^{-5}{*}D^2 - 4.60(10)^{-7}{*}P^2 - 7.72(10)^{-6}{*}D{*}P \quad \text{(Eq 5)}$$

$$\text{Coal slag: } R_z = -3.40(10)^{-3} + 1.02(10)^{-3}{*}D + 1.27(10)^{-4}{*}P + 1.10(10)^{-5}{*}D^2 - 4.60(10)^{-7}{*}P^2 - 7.72(10)^{-6}{*}D{*}P \quad \text{(Eq 6)}$$

$$\text{Chilled iron: } R_z = -1.52(10)^{-3} + 7.37(10)^{-4}{*}D + 1.14(10)^{-4}{*}P + 1.11(10)^{-5}{*}D^2 - 4.60(10)^{-7}{*}P^2 - 7.72(10)^{-6}{*}D{*}P \quad \text{(Eq 7)}$$

where D is the blast distance in cm and P is the blast pressure in kPa.

3. Coating Adhesion Study

Aluminum and Zn-Al coatings were applied to substrates prepared using the grit materials of this study. The TWEA spray process was chosen for this application since it has been used for many bridge applications. The process is capable of producing relatively low-porosity coatings with high bond strength.

3.1 Experimental Procedure

A Praxair Tafa, Inc. (Concord, NH) Model 9000 TWEA spray system and commercially available wire (i.e., Praxair Tafa 01T aluminum and Praxair Tafa 02A 85Zn/15Al) were used. Aluminum coatings were first sprayed onto A36 steel substrates roughened with the HG16 steel grit. A central composite response surface design of experiment was used, varying spray parameters of current, pressure, and spray distance in 17 experiments. Optimum grit-blast parameters were used for the HG16 grit. Twenty-one classic experiments were then conducted for the spraying of Zn-Al coatings on A36 steel using all seven of the grit materials of this study. Optimum grit-blast parameters were used for each grit material. Zinc-aluminum coatings were

Table 3 Aluminum/HG16 bond strength experiments

	Distance		Current	Pressure		Bond strength	
E No.	cm	in.	amp	kPa	psia	kPa	psia
1	7.62	3	100	275.8	40	12,086	1753
2	17.8	7	100	275.8	40	14,334	2079
3	7.62	3	300	275.8	40	15,182	2202
4	17.8	7	300	275.8	40	15,741	2283
5	7.62	3	100	551.6	80	12,645	1834
6	17.8	7	100	551.6	80	12,645	1834
7	7.62	3	300	551.6	80	15,458	2242
8	17.8	7	300	551.6	80	15,182	2202
9	5.08	2	200	413.7	60	13,769	1997
10	20.3	8	200	413.7	60	16,589	2406
11	12.7	5	100	413.7	60	12,645	1834
12	12.7	5	325	413.7	60	16,589	2406
13	12.7	5	200	208.2	30	15,741	2283
14	12.7	5	200	620.5	90	15,182	2202
15	12.7	5	200	413.7	60	16,306	2365
16	12.7	5	200	413.7	60	16,589	2406
17	12.7	5	200	413.7	60	14,899	2161

then sprayed onto the prepared substrates with standard spray parameters. Finally the bond strength of the TWEA sprayed coatings was then measured using a PATTI3 (Pneumatic Adhesion Tensile Testing Instrument, SEMicro, Rockville, MD) (Ref. 13).

3.2 Bond Strength of Al Coatings

Table 3 illustrates the SDE for the Al coatings applications using the substrate prepared HG16 steel grit. A response surface central composite SDE was conducted using a quadratic design model. Each variable has two levels selected to band around the nominal settings (i.e., experiments 1 through 8). Center-point experiments (i.e., 13 through 17) were also included to independently evaluate the process variation. The coatings were applied to the substrates within 2 h of grit blasting. The prepared substrates were visually examined with a Nikon (Nikon Corp., Japan) SMZ-2B microscope to inspect for surface contamination prior to spraying.

The process parameters included orifice diameter (green nozzle cap = 0.767 cm, or 0.302 in.), system pressure (P), amperage (A), and spray distance (D). Air was used as the primary and shroud gas (i.e., 208.2 kPa, or 30 psia). Wire injection was internal to the gun and directed parallel to the flow. Wire feed rate varies proportionally with the system current. The wire feed rates were 2.3 kg/h (5.1 lb/h) at 100 A, 4.0 kg/h (8.9 lb/h) at 200 A, and 6.7 kg/h (14.7 lb/h) at 300 A for the Al experiments; and 7.9 kg/h (17.3 lb/h) at 100 A, 16.6 kg/h (36.5 lb/h) at 200 A, and 25.3 kg/h (55.8 lb/h) at 300 A for the Zn-Al experiments. An x-y servomanipulator ensured the accuracy of the standoff distance and repeatability in the experiments. The traverse x-motion rate was 40.64 cm/s (16 in./s). A y-step of 0.635 cm (0.25 in.) was used. The wire was thermal sprayed onto A36/1020 low-carbon steel coupons (10.16 × 15.24 × 0.3175 cm, or 4 × 6 × 0.125 in.). The substrates were cooled by air jets on the backside to ensure a substrate temperature of approximately 93 °C (200 °F). The surface temperature was measured with a Raytek Raynger 3i portable IR temperature measurement device (Raytek Corp., Santa Cruz, CA). The deposition side of each coupon was grit blasted with HG16 steel grit at a 7.62 cm (3 in.) working distance

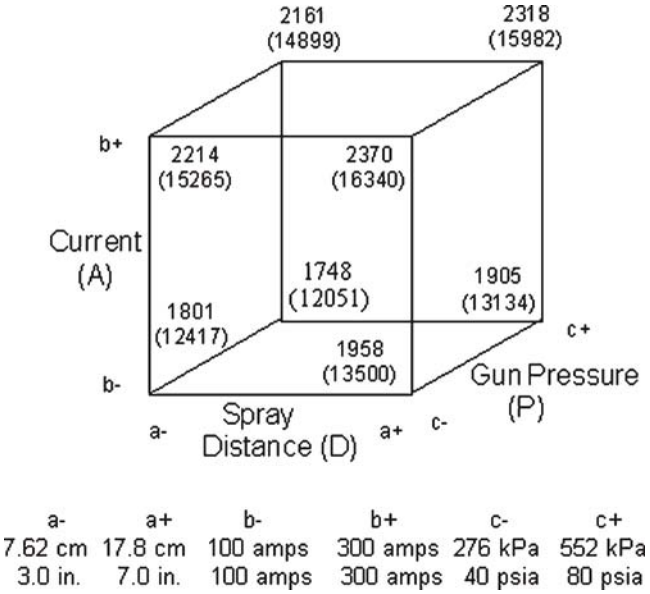

Fig. 4 Aluminum bond strength for HG16 grit

and 689.5 kPa (100 psia) pressure to obtain the maximum R_z profile (0.01 cm, or 3.9 mils).

Bond strength measurements were conducted using the PATTI3 adhesion tensile testing instrument. This instrument follows the test procedure described by ASTM standard D 4541 (Ref 14). The PATTI3 uses compressed inert gas to apply a continuous tensile load to a 1.27 cm (0.5 in.) diam Al pull stub, which is bonded to the test surface with 3M Scotch Weld Epoxy Adhesive 2214 (St. Paul, MN). This adhesive is a one-part, high-strength, gray-colored epoxy adhesive used to bond metals. Once the pull stub has been bonded and the adhesive has cured, a continuous load is applied perpendicular to the pull stub until failure occurs. The bond strength ranged from 12,086 to 16,589 kPa (1753 to 2406 psia) for the Al coatings sprayed onto substrates prepared using the HG16 grit.

As with the statistical analysis in the roughness study, effects and ANOVA analyses were conducted for bond strength. The I percent (I%) calculation indicates the influence of a factor or parameter on the measured response, with a larger number indicating more influence. The ANOVA calculations guide further experimentation by indicating which parameters are the most influential on coating attributes. High bond strength was most influenced in order by current, spray distance, and pressure. Higher current results in higher bond strength for the coatings as dictated by an I% of 66.4%, while higher spray distance had a I% of 25.2%, and lower pressure had an I% of 8.4%. The cube plot in Fig. 4 illustrates the bond strength values for the combinations of the upper and lower levels of the three selected processing variables for the Al coating study.

The regression equation for bond strength (kPa) for the Al coatings fabricated in this study using HG16 steel grit is:

$$\text{Al bond strength (HG16 grit)} = 3518.2 + 457.3*D + 59.55*A + 8.6*P - 13.78*D^2 - 0.113*A^2 - 0.012*P^2 \quad \text{(Eq 8)}$$

where D is the spray distance in cm, P is the spray pressure in kPa, and A is the spray gun current in amps.

Table 4 Zinc-aluminum coating bond strength for all 7 grit media

	Bond strength					
Grit type	kPa	psia	kPa	psia	kPa	psia
HG16	8342	1210	7819	1134	8481	1230
HG18	8342	1210	7819	1134	8057	1169
HG25	7634	1107	7634	1107	8203	1190
HG40	9050	1313	8203	1190	8203	1190
Cu slag	6364	923	7350	1066	6787	984
Coal slag	6926	1005	6926	1005	7350	1066
Chilled iron	3387	491	3387	491	4095	594

3.3 Bond Strength of Zn-Al Coatings

A comparison of the effect on bond strength as a function of the type of grit used in this study was conducted. Zinc-aluminum coatings were deposited on A36 steel substrates prepared using each of the seven grits with the grit-blast parameters that produced the roughest surface (maximum R_z and R_a values). Substrate roughness obtained for each grit type was consistent with the data illustrated in Fig. 2 and 3. Three bond strength tests were conducted for each grit type; the results are listed in Table 4. Zinc-aluminum coatings prepared using the HG grits exhibited higher bond strength than Cu slag, coal slag, and chilled Fe. Chilled Fe grit yielded the poorest adhesion strength, with average adhesion strength only 40% of that obtained using the HG grits.

4 Summary and Conclusions

An experimental study of grit blasting investigated included blast media, blast pressure, and working distance. Box-type statistically designed experiments were conducted on the effect of abrasives on roughness for A36/1020 steel. Surface profilometry was used to measure the surface texture parameters of the substrates. Surface texture was correlated with operating parameters. TWEA coatings were then deposited on the grit-blasted substrates. These coatings were then tested for bond strength using a portable adhesion tester following the test procedure described by ASTM standard D 4541.

The HG16, HG18, and HG25 steel grits used in this study produced higher substrate roughness parameters than Cu slag, coal slag, and chilled Fe grit. The HG16 steel grit produced the maximum R_z roughness, followed by HG18 steel, HG25 steel, Cu slag, coal slag, HG40 steel, and chilled Fe grit. Trend analysis indicated the R_z roughness increased at intermediate pressure (i.e., ~689.5 kPa, or 100 psia) and as working distance increased. The HG16 grit obtained the maximum R_a roughness, followed by HG18, HG25, HG40, Cu slag, coal slag, and chilled Fe grit. R_a roughness increased as the working distance and pressure increases, with the R_a roughness reaching a maximum at maximum pressure and distance. The trends evidenced for R_z and R_a are also witnessed for the parameters R_q, R_{3z}, R_t, R_y, and $R_{p\ max}$. The HG16 grit yielded higher measured values than the competing grits for all of these surface texture parameters except P_c. The measured values for P_c, the profile density, indicated higher values for smaller grit sizes.

Bond strength was measured using a PATTI3 portable adhesion tester. The bond strength ranged from 12,086 to 16,589 kPa (1753 to 2406 psia) for the Al coatings sprayed onto HG16 grit-blasted surfaces. Effects analysis indicated that high bond strength was most influenced, in order, by higher current, longer spray distance, and lower pressure. Zn-Al coatings were deposited on substrates prepared using seven grit materials with their optimum grit blast parameters. These coatings were tested for bond strength. The highest bond strengths were obtained on substrates roughened using the HG metal grit.

Acknowledgments

This work was funded by the Missile Defense Agency under the Small Business Innovation Research program. Analysis performed in collaboration with the Idaho National Laboratory was funded under DOE Contract DE-AC07-05ID14517. References herein to any specific commercial product, process, or service by trade name, trademark, manufacturer, or otherwise, do not necessarily constitute or imply its endorsement, recommendation, or favoring by the U.S. Government, any agency thereof, or any company affiliated with the Idaho National Laboratory.

References

1. *Properties and Selection: Nonferrous Alloys and Special-Purpose Materials,* Vol 2, *ASM Handbook,* ASM International, 1991
2. C.C. Berndt and C.K. Lin, Measurement of Adhesion for Thermally Sprayed Materials, *J. Adhes. Sci. Technol.,* 1993, **7**(12), p 1235-1264
3. *Engineering and Design—Thermal Spraying: New Construction and Maintenance,* Engineer Manual EM 1110-2-3401, U.S. Army Corps of Engineers, Jan 1999
4. J.R. Davis, *Handbook of Thermal Spray Technology,* ASM International, 2004
5. M.F. Bahbou, P. Nylen, and J. Wigren, Effect of Grit Blasting and Spraying Angle on the Adhesion Strength of a Plasma-Sprayed Coating, *J. Therm. Spray Technol.,* 2004, **13**(4), p 508-514
6. R.A. Fisher, *The Design of Experiments,* 1st ed., Oliver and Boyd, Edinburgh, 1935
7. C.G., Pfeifer, Planning Efficient and Effective Experiments, *Mech. Eng.,* May 1988
8. *Econoline Manual RA 36-1,* Econoline Abrasive Products Division, Grand Haven, MI
9. G.E.P. Box, W.G. Hunter, and J.S. Hunter, *Statistics for Experimenters: An Introduction to Design, Data Analysis, and Model Building,* John Wiley and Sons, New York, 1978
10. P., Whitcomb, et al., *Design-Expert,* Stat-Ease Inc., Minneapolis, MN
11. Surftest 301 Surface Roughness Tester Manual No. 4648M Series No. 178, Mitutoyo Corp., Japan
12. "Surface Texture (Surface Roughness, Waviness, and Lay)," ASME B46.1-2002, The American Society of Mechanical Engineers, New York, 2003
13. PATTI3, Instruction Manual, SEMicro, Rockville, MD
14. "Standard Test Method for Pull-Off Strength of Coatings Using Portable Adhesion Testers," D 4541-02, *Annual Book of ASTM Standards,* Vol 06.02, Feb 2004